



Oxygen Effects in Anaerobic Digestion

Deshai Botheju Bernt Lie Rune Bakke

Faculty of Technology, Telemark University College, Kjølnes Ring 56, 3901, P.O. Box 203, N-3901 Porsgrunn, Norway; E-mail: Deshai.Botheju@hit.no

Abstract

Free oxygen effects in bio-gasification are not well known, apart from the common understanding of oxygen being toxic and inhibitory for anaerobic micro-organisms. Some studies have, however, revealed increased solubilisation of organic matter in the presence of some free oxygen in anaerobic digestion. This article analyses these counterbalancing phenomena with a mathematical modelling approach using the widely accepted biochemical model ADM 1. Aerobic oxidation of soluble carbon and inhibition of obligatory anaerobic organisms are modelled using standard saturation type kinetics. Biomass dependent first order hydrolysis kinetics is used to relate the increased hydrolysis rate with oxygen induced increase in biomass growth. The amended model, ADM 1-Ox (oxygen), has 25 state variables and 22 biochemical processes, presented in matrix form. The computer aided simulation tool AQUASIM 2.1 is used to simulate the developed model. Simulation predictions are evaluated against experimental data obtained using a laboratory batch test array comprising miniature anaerobic bio-reactors of 100 ml total volume each, operated under different initial air headspaces giving rise to the different oxygen loading conditions. The reactors were initially fed with a glucose solution and incubated at 35 °C for 563 hours. Under the oxygen load conditions of 22, 44 and 88 mg/L, the ADM1-Ox model simulations predicted the experimental methane potentials quite adequately. Both the experimental data and the simulations suggest a linear reduction of methane potential with respect to the increase in oxygen load within this range.

Keywords: anaerobic digestion, ADM 1, modelling, oxygen, simulation

1 Introduction

Conventionally the anaerobic digestion (AD) process should occur in a strict anaerobic environment with no free oxygen available. It is however not realistic to avoid all supply of free oxygen into anaerobic digester systems, and hence they can be exposed to considerable oxygen loads (Liden et al., 1994). Such aerobic invasions can deteriorate the performance of digestion systems (Hedrick et al., 1991); but the experience also shows the possibility of maintaining high methane generation activity with significant aerobic loads (Botheju et al., 2010). Improved performances under mild aerobic conditions in AD are also observed (Pirt and Lee, 1983; Gerritse et al., 1990; Johansen and Bakke, 2006; Zhou et al., 2007; Polanco et al., 2009). According

to the study by Pirt and Lee (1983), higher methane yield was observed in the digestion of algal biomass under oxygen limiting conditions. A similar observation was reported by Gerritse et al. (1990). Johansen and Bakke (2006) reported 50 % higher hydrolysis under micro-aerated anaerobic conditions. Successful use of limited aeration for toxic sulfide removal in anaerobic digesters fed with S containing wastes was confirmed by Zhou et al. (2007) and Polanco et al. (2009).

This study is an attempt to explain the dynamics of free oxygen in AD with a mathematical modeling approach. The aim is to develop a model basis for analyzing these aerobic-anaerobic interactions by exploiting the latest knowledge base on biochemical reactions related to aerobic and anaerobic wastewater treatment. The model predictions are further compared against

experimental data obtained in a laboratory batch test array where the variation of methane potential due to different air headspaces is observed.

2 Oxygen effects – theoretical and experimental basis

Anaerobic digestion is the totality of the collective interaction of at least three main microbial groups which are known as acidogens (acid generating biomass), acetogens (acetate generating biomass) and methanogens (methane generating biomass). Acidogenic organisms are the commonly known fermentative organisms which can ferment simple organic substrates in the absence of oxygen. The vast majority of this group of organisms are, however, facultative organisms (i.e. can thrive under either anaerobic or aerobic environments), implying that they can also use oxygen as electron acceptor. They tend to prefer oxygen and do aerobic respiration whenever oxygen is available, as it is energetically favourable. When the oxygen level is sufficiently low they may switch back to their normal fermentation mode for energy needs. The consumption of oxygen and readily available carbon sources, growth rates and conversion into carbon dioxide and other products are well studied and standard kinetic and stoichiometric parameters are available (Henze et al., 1995, 2002).

Macromolecular complex organic matter such as carbohydrates, proteins and fatty acids (the three main feed categories in AD) must be broken down into smaller soluble molecules to be consumed by acidogenic organisms. This process is commonly known as hydrolysis (solubilization) and is carried out by acidogenic microorganisms using their extra cellular enzymes. Hydrolysis can occur under both aerobic and anaerobic conditions. Hydrolysis rates are observed to be significantly higher under aerobic conditions, probably due to higher production of enzymes.

Acetogenic and methanogenic organisms are collectively responsible for the final conversion of acidogenesis products (volatile fatty acids) into a mixture of carbon dioxide and methane (biogas). These two groups of organisms are obligate anaerobes (i.e. can only survive under anaerobic conditions) and hence free oxygen can inhibit their functioning and can even lead to rapid cell lysis (annihilation of biomass).

An experimental series testing oxygen effects in AD (Johansen and Bakke, 2006) found that oxygen can enhance the hydrolysis stage, while higher oxygen levels cause more of the available soluble carbon to be oxidized into carbon dioxide (catalyzed by facultative acidogens), reducing the methane potential of the system. These observations suggest that an optimized

level of oxygen can enhance the digester performance by enhancing hydrolysis while minimizing inhibition of obligate anaerobes.

The model development described below is based on the above mentioned main facts and findings regarding oxygen effects in anaerobic digestion.

3 Model development

The model is developed using the generally accepted anaerobic digestion model ADM 1 structure (Batstone et al., 2002) which is developed by the Mathematical Modelling Task Group of the International Water Association (IWA). The ADM 1 contains 19 processes and 12 soluble components and 12 particulate components (i.e. 24 states). The ADM 1-Ox extension proposed includes the incorporation of oxygen as one extra soluble component, three additional aerobic uptake processes and oxygen effects on process kinetics.

3.1 Stoichiometric matrix and rate equations

The stoichiometric matrix for soluble components of the proposed ADM 1-Ox model is shown in Table 1. The new processes $j8$, $j9$ and $j10$ represent the aerobic uptake of monosaccharides, amino acids and long chain fatty acids (LCFA), respectively. Note that ADM 1-Ox does not introduce any new microbial groups in addition to the 7 groups already present in ADM 1. All three aerobic uptake processes are associated with the existing three acidogenic groups namely monosaccharide degraders (X_{su}), amino acid degraders (X_{aa}) and LCFA degraders (X_{fa}). It has been found that small aeration effects induce negligible impact on the phylogenetic diversity (diversity of species) of anaerobic digesters (Tang et al., 2004). Dissolved oxygen concentration (S_{O_2}) is introduced as a new soluble component ($i12$). The selected unit for oxygen in the model is kgO_2/m^3 . The aerobic uptake rates are described using Monod saturation type (Monod, 1949) kinetic equations shown in Equations (1-3). Other biochemical rate expressions in ADM 1-Ox also utilize Monod type kinetics.

$$r_{aer, su} = k_{m, su} \left(\frac{S_{su}}{K_{s, su, aer} + S_{su}} \right) \left(\frac{S_{o_2}}{K_{o_2} + S_{o_2}} \right) X_{su} I_1 \quad (1)$$

$$r_{aer, aa} = k_{m, aa} \left(\frac{S_{aa}}{K_{s, aa, aer} + S_{aa}} \right) \left(\frac{S_{o_2}}{K_{o_2} + S_{o_2}} \right) X_{aa} I_1 \quad (2)$$

$$r_{aer,fa} = k_{m,fa} \left(\frac{S_{fa}}{K_{s,fa,aer} + S_{fa}} \right) \left(\frac{S_{o2}}{K_{o2} + S_{o2}} \right) X_{fa} I_2 \quad (3)$$

Integrated inhibition term I_1 includes 2 inhibition type terms used in ADM 1 for describing microbial inhibition due to extreme pH conditions and limitation of soluble inorganic nitrogen. Inhibition term I_2 in Equation (3) is the resultant of multiplying I_1 with one more inhibition term representing the hydrogen inhibition of LCFA degrading organisms. An additional inhibition term, I_{O_2} , is introduced in ADM 1-Ox to account for oxygen inhibition effects on the strictly anaerobic acetogens and methanogens. A generally accepted non-competitive type inhibition function was used as a gradual oxygen switch (Equation (4)). The same oxygen inhibition function was also used to account for negative effects of oxygen on fermentation / acidogenesis rates (Table 1).

$$I_{O_2} = \frac{K_{O_2}}{K_{O_2} + S} \quad (4)$$

3.2 Oxygen stoichiometry

Stoichiometric coefficients for oxygen under aerobic uptake processes were approximated using representative chemical formula for 3 basic substrates (carbohydrates – $C_{10}H_{18}O_9$; lipids – $C_8H_6O_2$; protein – $C_{14}H_{12}O_7N_2$) (Henze et al., 2002). Three new yield coefficients were introduced to represent the additional biomass growth under oxygen respiration. Then the total yields of three acidogenic biomass groups are the additions of anaerobic and aerobic yields (stoichiometric matrix for the particulate components is not shown here). Aerobic growth of 3 acidogenic groups lead to additional inorganic nitrogen assimilation and is taken into account by the products of their aerobic yields and biomass nitrogen content. Different to the fermentation processes which can produce multiple products, aerobic uptake results in oxidation of substrates into the single product of carbon dioxide (besides cell growth). Hence the averaged carbon content values (as $kmol$ carbon per kg Chemical Oxygen Demand, $kmol C/kg COD$) of the three substrate groups ($C_1 = 0.03125$ for sugars, $C_2 = 0.030$ for amino acids and $C_3 = 0.0217$ for LCFAs) can directly be used together with respective aerobic yield coefficients as the stoichiometric coefficients under inorganic carbon (IC) balance (component $i10$, Table 1).

3.3 Hydrolysis rates

Standard ADM 1 uses first order rate expressions of the form in Equation (5) to represent hydrolysis, not

taking the effect of acidogenic biomass concentration on hydrolysis into account. Oxygen can, however, be expected to enhance hydrolysis through aerobic growth and higher biomass concentration. This effect but not this mechanism can be included by just increasing the hydrolysis rate constant (K_{hyd}). A more mechanistic hydrolysis model is chosen in ADM 1-Ox by using the modified first order rate expressions which include biomass concentration terms. The kinetic expressions for hydrolysis of carbohydrates (ch), proteins (pr) and lipids (li), in processes $j2$, $j3$ and $j4$, are modified accordingly (Equations (6 -8)). Note that the hydrolysis of ch , pr and li are catalysed by respective acidogenic biomass groups X_{su} , X_{aa} and X_{fa} which utilize the relevant hydrolytic products.

$$r_{hyd,x} = k_{hyd,x} X_x \quad (5)$$

$$r_{hyd,ch} = k_{hyd,ch} X_{ch} X_{su} \quad (6)$$

$$r_{hyd,pr} = k_{hyd,pr} X_{pr} X_{aa} \quad (7)$$

$$r_{hyd,li} = k_{hyd,li} X_{li} X_{fa} \quad (8)$$

3.4 Kinetic and stoichiometric parameters

The simulations carried out with ADM 1-Ox use a typical set of kinetic parameters suggested in the standard ADM 1 model (Batstone et al., 2002). The few new oxygen related kinetic constants in ADM 1-Ox are estimated or chosen by comparing mainly three sources: ADM 1 kinetics parameter list (Batstone et al., 2002), ASM 2 kinetic parameter list (Henze et al., 1995) and Henze et al. (2002). Accordingly the three aerobic yield coefficients are given the values of $Y_{su,aer} = 0.5$; $Y_{fa,aer} = 0.3$; $Y_{aa,aer} = 0.4$ (in $kg COD$ biomass per $kg COD$ substrate metabolized).

Saturation coefficients (K_s) under aerobic condition are set to be one fifth of the values used under anaerobic conditions in ADM 1. This is in agreement with the used K_s values in the ASM 2 model under aerobic and anaerobic conditions. Therefore the used values are $K_{s,aa,aer} = 0.06$; $K_{s,fa,aer} = 0.08$; $K_{s,su,aer} = 0.1$ (in the units of $kg COD/m^3$).

A calculation based on the formula, $K_m = \mu^{max}/Y$ shows that the ratio of K_m values under aerobic and anaerobic (fermentative) conditions is close to 0.9 (or ~ 1). Then by considering also the uncertainty of these parameters it is decided to use the same values under both conditions.

The oxygen inhibition parameter K_{O_2} in Equation (4) is given the same value as the half saturation constant for oxygen in aerobic uptake processes, as in the ASM 2 model (Henze et al., 1995). All three hydrolysis rate constants (K_{hyd}) are adjusted by one order of magnitude in order to compensate for the modification done to the hydrolysis rate equations.

Table 1: Stoichiometric matrix of the ADM1-Ox Model for soluble components.

Component, i	$i1$	$i2$	$i3$	$i4$	$i5$	$i6$	$i7$	$i8$	$i9$	$i10$	$i11$	$i12$	$i13$	Rate (ρ_j) [kgCOD/m ³ · d]
Processes, j	S_{su}	S_{su}	S_{fa}	S_{su}	S_{su}	S_{pro}	S_{ac}	S_{a2}	S_{ch4}	S_{IC}	S_{IN}	SO_2	S_I	
$j1$. Dis-integration													F_{slac}	$K_{dis} X_c$
$j2$. Hydrolysis of Carbohydrates	1													$K_{hyd} ch X_{ch} X_{su}$
$j3$. Hydrolysis of proteins		1												$K_{hyd} pr X_{pr} X_{su}$
$j4$. Hydrolysis of lipids	$-F_{fat}$		F_{fat}											$K_{hyd} li X_{li} X_{su}$
$j5$. Sugars uptake	-1				$(1 - Y_{su}) F_{hu,su}$	$(1 - Y_{su}) F_{pro,su}$	$(1 - Y_{su}) F_{ac,su}$	$(1 - Y_{su}) F_{h2,su}$						$K_{m,su} \frac{S_{su}}{K_{s,su} + S_{su}} X_{su} I_1 I_2$
$j6$. Amino acids uptake		-1		$(1 - Y_{su}) F_{hu,aa}$	$(1 - Y_{su}) F_{hu,aa}$	$(1 - Y_{su}) F_{pro,aa}$	$(1 - Y_{su}) F_{ac,aa}$	$(1 - Y_{su}) F_{h2,aa}$						$K_{m,aa} \frac{S_{su}}{K_{s,aa} + S_{su}} X_{su} I_1 I_2$
$j7$. LCFA uptake			-1				$(1 - Y_{fa}) 0.7$	$(1 - Y_{fa}) 0.3$						$K_{m,fa} \frac{S_{fa}}{K_{s,fa} + S_{fa}} X_{fa} I_1 I_2$
$j8$. Aerobic uptake of sugar	-1									$C_1 (1 - Y_{su, aer})$	$-Y_{su, aer} N_{huac}$	-1.1		$K_{m,su} \frac{S_{su}}{K_{s,su} + S_{su}} \frac{S_{O_2}}{K_{O_2} + S_{O_2}} X_{su} I_1$
$j9$. Aerobic uptake of aminoacids		-1								$C_2 (1 - Y_{aa, aer})$	$\frac{N_{aa}}{Y_{aa, aer} N_{huac}}$	-1.2		$K_{m,aa} \frac{S_{su}}{K_{s,aa} + S_{su}} \frac{S_{O_2}}{K_{O_2} + S_{O_2}} X_{su} I_1$
$j10$. Aerobic uptake of LCFA			-1							$C_3 (1 - Y_{fa, aer})$	$-Y_{fa, aer} N_{huac}$	-2.03		$K_{m,fa} \frac{S_{fa}}{K_{s,fa} + S_{fa}} \frac{S_{O_2}}{K_{O_2} + S_{O_2}} X_{fa} I_2$
$j11$. Uprake of valerate				-1		$(1 - Y_{cd}) 0.54$	$(1 - Y_{cd}) 0.31$	$(1 - Y_{cd}) 0.15$			$-Y_{cd} N_{huac}$			$K_{m,cd} \frac{S_{huac}}{K_{s,cd} + S_{huac}} X_{cd} \frac{1}{1 + S_{huac}/S_{su}} I_2 I_2$
$j12$. Uprake of butyrate					-1		$(1 - Y_{cd}) 0.8$	$(1 - Y_{cd}) 0.2$			$-Y_{cd} N_{huac}$			$K_{m,cd} \frac{S_{huac}}{K_{s,cd} + S_{huac}} X_{cd} \frac{1}{1 + S_{huac}/S_{su}} I_2 I_2$
$j13$. Uprake of propionate						-1	$(1 - Y_{pro}) 0.57$	$(1 - Y_{pro}) 0.43$			$-Y_{pro} N_{huac}$			$K_{m,pro} \frac{S_{huac}}{K_{s,pro} + S_{huac}} X_{pro} I_2 I_2$
$j14$. Uprake of acetate							-1		$1 - Y_{ac}$		$-Y_{ac} N_{huac}$			$K_{m,ac} \frac{S_{huac}}{K_{s,ac} + S_{huac}} X_{ac} I_2 I_2$
$j15$. Uprake of hydrogen								-1	$1 - Y_{h2}$		$-Y_{h2} N_{huac}$			$K_{m,h2} \frac{S_{huac}}{K_{s,h2} + S_{huac}} X_{h2} I_1 I_2$
$j16$ - $j22$. Biomass decay processes														$K_{dis} X_i, i = 18 - 24$

4 Methodology

4.1 Experimental

An experimental test array was established to test the methane potential under different initial oxygen loading conditions. *BDPlastipak* 100 ml polypropylene syringes (supplied by VWR International), transformed into miniature bio-reactors, were used to carry out the experimentation for 563 hours duration (23.5 days) incubated at 35 °C. After filling the syringes with the inoculum together with the substrate up to the 50 ml volume mark, hypodermic needles were attached. Each needle was then inserted into a rubber stopper to close and isolate the system. As gas is produced the piston is displaced outwards and the produced biogas volume is read on the scale. After 563 hours, the observed gas generation had stopped. The reactors were initially provided with different air headspace displacements of 0, 4, 8, and 16 ml to introduce different oxygen loading conditions. Triplicates of reactors were used for each test condition and the measurement and analysis results were averaged for final evaluation. The test reactors were fed with 1 ml of 0.5 M glucose solution at the start up of the experiment (equivalent to an initial substrate concentration of 1.92 kg COD/m³). Control reactors without feeding were also included in order to quantify the gas generation potential of the inoculum alone.

The inoculum used here was taken from an active municipal anaerobic digester treating wastewater sludge (*Knarrdalstrand* municipal wastewater treatment facility, *Porsgrunn*, Norway). This digester is a completely mixed reactor operated at 35 °C and fed chemically precipitated primary sludge from municipal wastewater. The digester is preceded by a micro-aerobic contactor with a short hydraulic retention time (< 24 h). The inoculum was stored at room temperature for 30 days in order to deplete the remaining degradable substrate from the wastewater before used in the experiment. This ensures minimum gas generation due to remaining substrate in the inoculum (Fig. 1a), making it easier to distinguish the most relevant experimental results and also simulate the process. Prior to being used in the batch test array, the inoculum was filtered through a 0.5 mm sieve to remove the larger particulate material. While filling the miniature reactors, the inoculum vessel was constantly mixed and de-aerated by nitrogen purging. The dissolved oxygen reading was below 0.35 mg/L.

4.2 Analytical methods

Measurements and analyses were conducted to determine gas generation, gas composition, soluble and total

COD, *pH*, *VFA* (volatile fatty acids including acetic, propionic, butyric and valeric), NH_4^+ , *TSS/VSS* (total/volatile suspended solids), *TS/VS* (total/volatile solids) and alkalinity. The total gas generation is measured daily (or twice a day at the beginning) by taking readings on the volumetrically labeled piston displacement. Gas composition analysis is carried out at three different occasions (140 hrs., 299 hrs. and 563 hrs.) during the course of the experiment using a Gas Chromatograph (*HewlettPackard* P series, micro GC) with helium as the carrier gas. Compositions of methane, carbon dioxide, nitrogen and oxygen were determined accordingly. Then the amount of methane gas generated was calculated based on the total gas volume. Liquid phase analyses were carried out according to the established standard test methods (*APHA et al., 1995*).

4.3 Oxygen loads

Table 2 summarizes the different oxygen loading conditions tested. Supplied oxygen mass in moles indicated in column 3 is obtained using the ideal gas law relation ($n = pv/RT$) at 298 K temperature (filling temperature of the headspaces) and 1 atm. pressure. The rightmost column indicates the corresponding oxygen load provided in the 50 ml reactor mixed liquor. These oxygen load values ($g O_2/m^3 = mg O_2/L$ reactor content) are consistently used here to describe the reactor oxygen loading conditions while elaborating the experimental and simulation results.

4.4 Oxygen transfer coefficients (k_La)

The following analysis is carried out to estimate the equivalent oxygen transfer coefficients (k_La) corresponding to the oxygen loads indicated in Table 2.

The rate of aeration can be expressed as,

$$\frac{dC}{dt} = k_La(C^* - C) \quad (9)$$

Here, C is the oxygen concentration and C^* represents the saturation oxygen concentration in the system. Assuming that the free oxygen concentration in the liquid phase is near zero due to rapid oxygen consumption by facultative biomass (*Botheju et al., 2009*), then Equation (9) can be re-arranged to give the oxygen mass transfer rate into the reactor,

$$\frac{dM}{dt} = V k_La C^* \quad (10)$$

Here V is the liquid volume of the reactor and M is the oxygen mass. It follows that,

$$\int dM = V k_La C^* \int dt + k_o \quad (11)$$

Table 2: Oxygen loading conditions tested in experiments and in simulations.

Initial air head space vol. (mL)	Initial O_2 vol. (mL)	Initial O_2 mass (mol) $\times 10^5$	Initial O_2 mass (mg)	Equivalent O_2 load (mg/L)
0	0	0	0	0
4	0.8	3.4	1.10	22
8	1.7	6.9	2.2	44
16	3.4	13.7	4.4	88

$$\Rightarrow M = V k_L a C^* t + k_o \quad (12)$$

Neglecting the initial oxygen content in the liquid phase, $k_o = 0$; hence,

$$k_L a = \frac{M}{V C^* t} \quad (13)$$

The M values are given in the 4th column of Table 2, and $V = 0.05 L$ (reactor liquid volume). For the approximation of “uniform aeration” of reactor liquor due to initial headspace, t may be taken as 23.5 days (experiment duration). It can be reasonably assumed that all the oxygen supplied through the headspaces is depleted during this time period.

Saturation oxygen concentration C^* is calculated according to the empirical formula by Weiss (1970). For zero salinity solutions,

$$\ln(C^*) = A_1 + A_2 \left(\frac{100}{T} \right) + A_3 \ln \left(\frac{100}{T} \right) + A_4 \left(\frac{100}{T} \right) \quad (14)$$

Here, T is the absolute temperature and the C^* is given in ml/L . The empirical constants have the values, $A_1 = -173.4292$; $A_2 = 249.6339$; $A_3 = 143.3483$; $A_4 = -21.8492$. From Equation (14), $C^* = 6.95 mg/L$ at 308K (operating temperature).

The equivalent $k_L a$ values (d^{-1}) corresponding to the different air headspaces are calculated according to Equation (13) and are given in Table 3. These $k_L a$ values were used in the ADM 1-Ox model simulations to represent the different oxygen loading conditions tested in the experiment.

 Table 3: Estimated $k_L a$ values.

Equivalent O_2 load (mg/L)	Equivalent $k_L a (d^{-1})$
0	0
22	0.14
44	0.27
88	0.54

4.5 Simulation method

The computer aided simulation tool AQUASIM 2.1 (Reichert, 1998) is used to simulate the developed ADM 1-Ox model under the operating conditions of the experimental trials described above. According to the preliminary simulations carried out before (Both-eju et al., 2009), it is observed that the low oxygen loading conditions such as oxygenated influent streams cannot cause significant detrimental effects in anaerobic digesters, primarily due to the rapid oxygen consuming ability of facultative acidogenic biomass. In order to include the prolonged aeration effect due to the air headspaces provided in the experimental trials analyzed here, a continuous aeration process is introduced in the model as an additional dynamic process. The aeration rate is described using an equivalent oxygen transfer coefficient ($k_L a$) and the oxygen concentration driving force ($C^* - C$). Each experimental oxygen loading condition is then simulated using a corresponding equivalent $k_L a$ value (Table 3). The applied glucose feed concentration ($1.92 kg COD/m^3$) is specified as the initial condition of the monosaccharide concentration in the simulation program. Initial conditions for the other degradable substrates were given diminutive values (putting them as zeros hinder the initialization of the simulator).

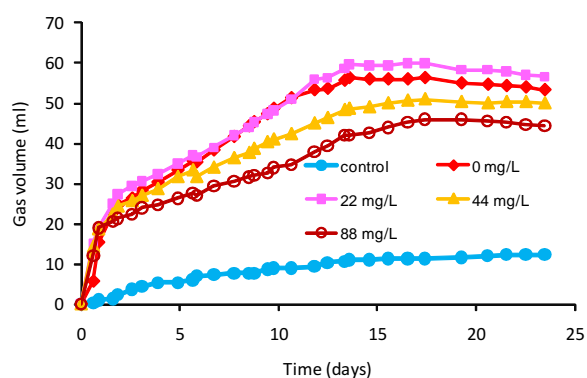
In order to simulate the cumulative gas generation in the AQUASIM built ADM 1-Ox model, the reactor headspace is defined as a variable volume completely mixed reactor. No kinetic parameters are modified or optimized from their values given in the original sources.

5 Results and discussion

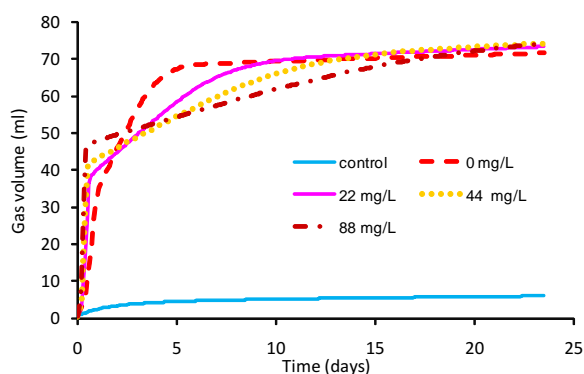
5.1 Total cumulative gas generation

Total cumulative biogas generation measured and simulated under the operating conditions investigated, are shown in Fig. 1a and Fig. 1b, respectively.

The experimental curves exhibit three distinguishable phases having markedly different gas generation rates (Fig. 1a): An initial high generation of short



(a) Experimental.



(b) Simulated.

Figure 1: Experimental (a) and simulated (b) total cumulative gas generation for the control and for different oxygen loading conditions.

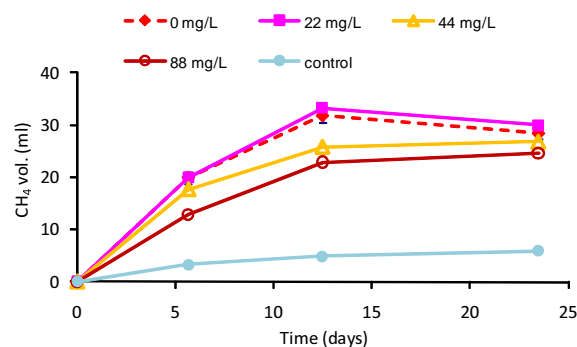
duration, an extended period of an approximately constant production rate, and eventually a final period of very low gas production. Simulation curves display a similar behavior (Fig. 1b) with the general order and the magnitudes of gas generation. Simulations, though somewhat over-predicts the total gas generation, still substantiate the experimentally shown exhaustion of gas generation within 20 days. The final total biogas production is on average approximately the same with and without oxygen loads. This can be expected, as the possible reduction in methane yield due to oxygen is compensated by increased CO_2 production. The oxygen appears to speed up the initial biogas production rate, observed both in the experiments and in the simulations. Oxygenation in AD can lead to reduced initial accumulation of volatile fatty acids (Botheju et al., 2010), due to aerobic VFA degradation. High VFA concentration inhibits and slows down the methanogenic phase of the digestion, a problem that can therefore be avoided with micro-aeration. This, together with increased CO_2 production, can lead to higher initial biogas generation rates observed under aerated condi-

tions. Nguyen et al. (2007) observed that pre-aerated anaerobic reactors reached the active methane phase ($> 50\%$ CH_4 in the biogas) quicker than completely anaerobic reactors.

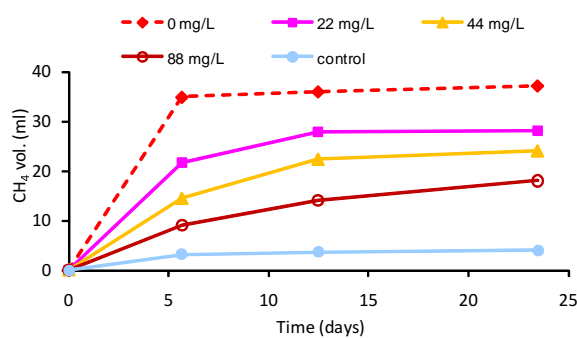
The experimental curves are not as congregated as the simulated ones. These deviations suggest that the standard model parameters applied do not fully account for all effects of oxygen in such processes.

5.2 Methane generation potential

The methane fractions of the produced biogas under different oxygen loading conditions, simulated and measured, are presented in Figures 2 and 3. The measured methane generations for different oxygen loading conditions are quite closely predicted by the model simulations (Figs. 3a – 3e).



(a) Experimental.



(b) Simulated.

Figure 2: Relative placement of methane generation curves under different oxygen loading conditions according to the experimental data and the simulation predictions.

According to the experimental data (Fig. 2a), 22 mg/L oxygen load only induce a minor (not statistically significant) impact on the methane generation potential, while 44 and 88 mg/L loads induced increas-

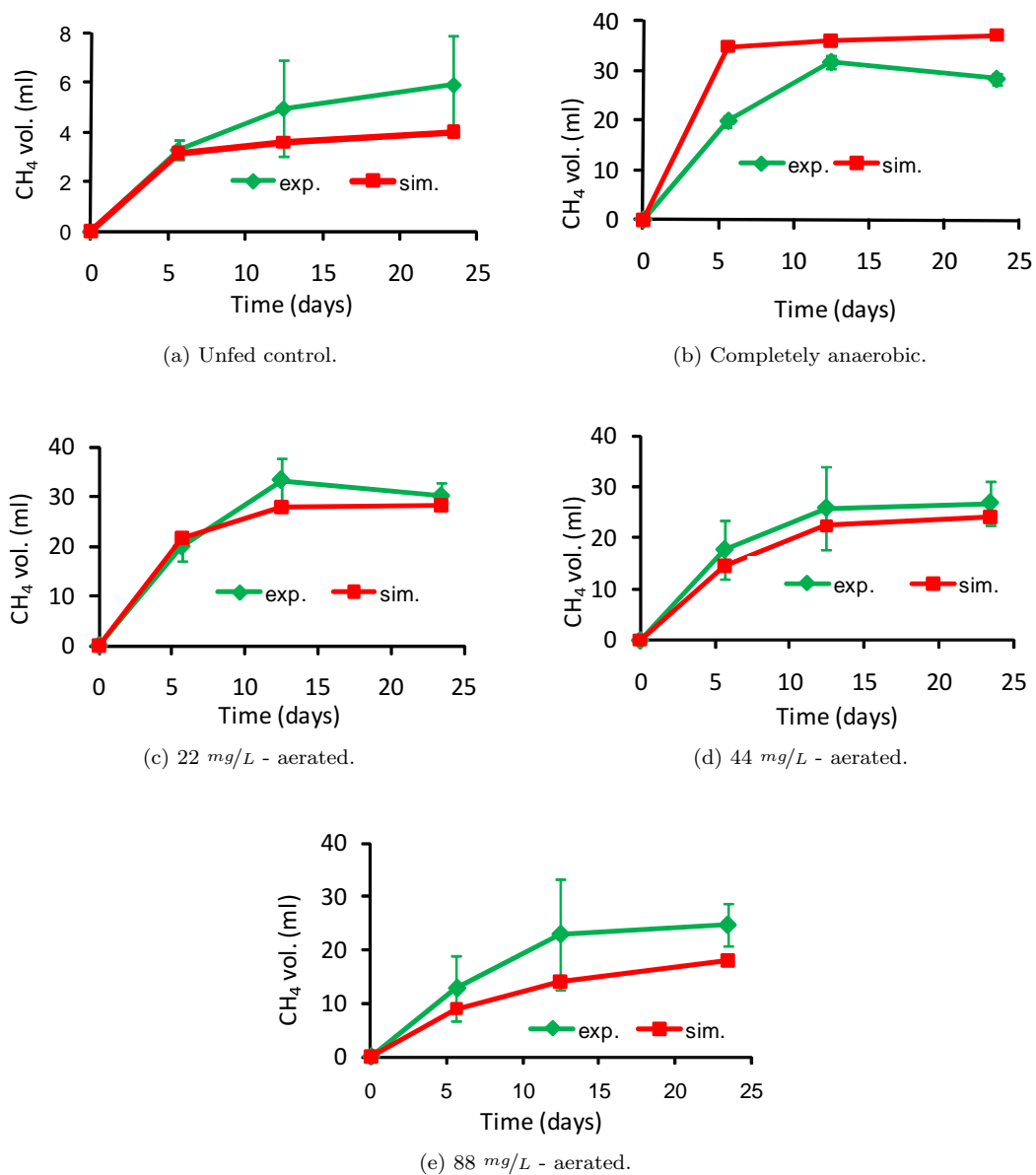


Figure 3: Cumulative methane generation measured in the control and in different air headspace experiments compared against simulation predictions.

ingly negative impacts on the methane potential. Simulations predict distinguishable and increasingly negative impacts on the methane generation potential at increasing oxygen loads (Fig. 2b). The deviations between the model predicted and experimental methane generation implies that the standard model parameters applied over-predict the negative impact of oxygen and/or underestimate the positive effects. It is also conceivable that some un-known oxygen effect has an impact. Further, observed over-prediction at zero oxygen condition could have been caused by the initial inoculum conditions which were not fully characterized.

Figure 4 displays experimental and model predicted ultimate methane generation against different oxygen loads. Though the model somewhat over-predicted the methane potential at zero oxygen load, it quite closely predicted the methane potential under the oxygen loads of 22, 44 and 88 mg/L cases.

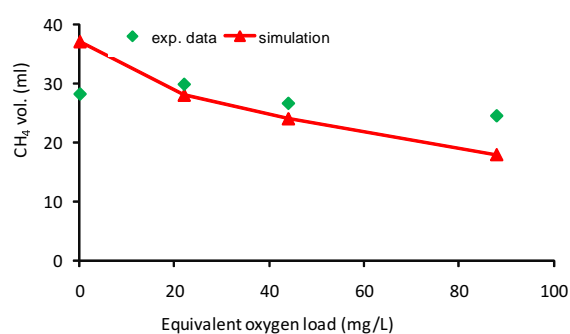


Figure 4: Experimentally determined and simulation predicted ultimate methane generation vs. oxygen load.

5.3 Linear reduction of methane potential

The experimental and simulated methane generation data at 22, 44 and 88 mg/L oxygen loads demonstrate a near linear decrease of methane potential with increasing oxygen load (Figure 5). The coefficients of determination (R^2) values for the experimental data (0.908) and simulated data (0.995) indicate above 90% confidence in linearity. The data point for zero oxygen condition does not fall within this linear region. Apparently, there is a certain non-linear behavior when the condition changes from fully anaerobic to oxygen affected methane generation. Both the experimental and simulated data suggest the existence of such a non-linearity at this transition region. If not for this initial non-linearity, then interestingly enough, the experimental and simulation lines have a similar intercept

on the ordinate axis suggesting the exact same value of methane potential at zero oxygen load (31.1 mL). This value is 16.4% below the simulation prediction for the zero oxygen condition and 9.5% above the experimentally determined value for zero oxygen load. The higher slope of the simulation line (0.15) compared to the experimental line (0.076) causes the simulation data to increasingly over-predict the negative impacts of increasing oxygen loads. This is consistent with, and explained in the section 5.2. Simulation curve fit to the experimental data can be improved by parameter estimation (including and perhaps especially the oxygen inhibition coefficient); but that is beyond the scope of this study.

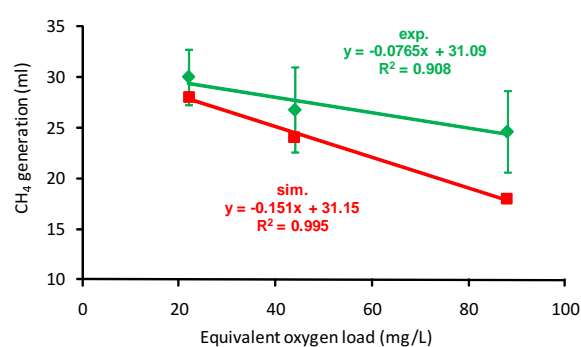


Figure 5: Analysis of linearity for experimental and simulated data in the 22 – 88 mg/L oxygen load range.

5.4 Rationale

The reduction of methane potential observed in experiments and in simulations can be attributed to the substrate oxidation by facultative acidogenic organisms and the partial inhibition of the activity of strictly anaerobic biomass. Since a soluble substrate is used (glucose), an increase in hydrolysis due to aerobic activity of facultative organisms cannot be expected. Previous studies indicated that even with the increased hydrolysis (~ 50% increase) due to micro-aeration, the ultimate methane yield has been reduced (by ~ 50%) (Johansen and Bakke, 2006). The effect of the enhanced hydrolysis can apparently be undermined by the rapid aerobic oxidation of hydrolytic products, caused by increased level of aeration.

Reduced methane yield under limited aeration conditions associated with substrate oxidation by aerobic respiration has also been observed by O'Keefe and Chynoweth (2000) in an experimental study on aeration effects in simulated landfill cells and by Mshandete et al. (2005) for digestion of sisal pulp waste. Aer-

obic substrate oxidation can also explain observations made by [Botheju et al. \(2010\)](#) where reduced soluble organic matter contents (measured as VFA and soluble COD) and reduced methane generation were observed in a semi-continuous digester fed a mixture of peptone, starch and yeast extract. The reduction in methane generation was linear with oxygen load. The methane generation was quickly resumed with reduced oxygen loads. These observations suggest that oxygen inhibition of methanogens was not a dominant factor causing reduced methane generation, while aerobic substrate consumption was. Oxygen inhibition was avoided due to the rapid oxygen consumption by facultative organisms under excess substrate conditions, thus effectively shielding obligatory anaerobes from oxygen exposure ([Kato et al., 1997](#)).

The use of simulation and experimental data discussed here are restricted to the specific operating conditions and oxygen load levels tested. However the general ability of the developed ADM 1-Ox model to predict oxygen impacts in anaerobic digestion is demonstrated based on this experimental study.

6 Conclusions

Effects of free oxygen in anaerobic digestion is modelled by expanding the standard ADM 1 model to also account for some known biochemical interactions of oxygen in an anaerobic/methanogenic environment.

The developed ADM 1-Ox model is successfully implemented and simulated in the AQUASIM 2.1 simulation tool. The developed model is evaluated based on laboratory batch test data. Under the experimental conditions tested (batch condition of 23.5 days, 1.92 kg COD/m^3 initial glucose feed concentration, $35 \text{ }^\circ\text{C}$ operating temperature, $0\text{--}88 \text{ mg/L}$ equivalent oxygen loading range), the developed ADM 1-Ox model can be used to predict the oxygen impact on anaerobic digestion with satisfactory results.

Experimental and simulation data suggest a linear decrease of methane potential at increasing oxygen loads under these operating conditions.

The proposed modeling approach can be utilized to understand and quantify oxygen impacts on anaerobic bio-gasification processes. It will be used to optimize aeration, to enhance the digestibility of recalcitrant and particulate organic matter through increased solubilization, while minimizing the observed negative impacts on methane generation.

Acknowledgment

This study is funded by grants from the Research Council of Norway. A special thank goes to Labo-

ratory Engineer at Telemark University College, Ms. Hildegunn H. Haugen, for her technical support.

Nomenclature

<i>aa</i>	amino acids
<i>ac/act/acet</i>	acetic, acetate
<i>bu/buty</i>	butyric, butyrate
<i>ch</i>	carbohydrates
<i>C</i>	oxygen concentration (mg/L)
<i>C*</i>	saturation concentration (mg/L)
<i>conc</i>	concentration
<i>d</i>	days (time unit)
<i>DO</i>	dissolved oxygen
<i>a/Fa/lcfa</i>	fatty acids /LCFA
<i>k_{hyd}</i>	first order hydrolysis rate constant
<i>k_m</i>	uptake rate constant
<i>k_s</i>	half saturation constant (Monod)
<i>k_{La}</i>	oxygen transfer coefficient (d^{-1})
<i>LCFA</i>	long chain fatty acids
<i>li</i>	lipids
<i>M</i>	oxygen mass (mg)
<i>pr</i>	protein
<i>pro/prop</i>	propionate, propionic
<i>r</i>	reaction rate
<i>r_{hyd}</i>	hydrolysis rate
<i>S</i>	conc. of a soluble component
<i>su/ms</i>	sugar/monosaccharides
<i>T</i>	absolute temperature (K)
<i>t</i>	time (days)
<i>V</i>	reactor liquid volume (L or mL)
<i>va/val</i>	valeric, valerate
<i>VFA</i>	volatile fatty acids
<i>x, X</i>	conc. of a particulate component
<i>X_{aa}</i>	amino acids degraders (biomass conc.)
<i>X_{ac}</i>	acetoclastic methanogens
<i>X_{c4}</i>	butyrate and valerate degraders
<i>X_{fa}</i>	LCFA degraders
<i>X_{h2}</i>	hydrogenotrophic methanogens
<i>X_{prop}</i>	propionate degraders
<i>X_{su}</i>	sugar (monosaccharide) degraders
<i>μ_{max}</i>	maximum specific growth rate

References

- APHA, AWWA, and WEF. *Standard methods for the examination of water and wastewater*. Washington DC, USA, 1995.
- Batstone, D. J., Keller, J., Angelidaki, I., Kalyuzhnyi, S., Pavlostathis, S. G., Rozzi, A., Sanders, W., Siegrist, H., and Vavilin, V. *Anaerobic digestion Model No.1*. IWA publishing, 2002.

- Botheju, D., Lie, B., and Bakke, R. Modeling free oxygen effects in anaerobic digestion. In *Proceedings of the MATHMOD 2009 - 6th Vienna International Conference on Mathematical Modeling, Vienna, 11-13 February*. 2009 .
- Botheju, D., Samarakoon, G., Chen, C., and Bakke, R. An experimental study on the effects of oxygen in bio-gasification; part 1 & part 2. In *Proceedings of the International Conference on Renewable Energies and Power Quality (ICRE PQ 10), Granada (Spain), 23-25 March*. 2010 .
- Gerritse, J., Schut, F., and Gottschal, J. C. Mixed chemostat cultures of obligately aerobic and fermentative or methanogenic bacteria grown under oxygen-limiting conditions. *FEMS Microbiology Letters*, 1990. 66:87 – 94. doi:[10.1111/j.1574-6968.1990.tb03977.x](https://doi.org/10.1111/j.1574-6968.1990.tb03977.x).
- Hedrick, D. B., Guckert, J. B., and White, D. C. The effects of oxygen and chloroform on microbial activities in a high-solids high-productivity anaerobic biomass reactor. *Biomass and Bioenergy*, 1991. 1(4):207 – 212. doi:[10.1016/0961-9534\(91\)90004-V](https://doi.org/10.1016/0961-9534(91)90004-V).
- Henze, M., Gujer, W., Mino, T., Matsuo, T., Wentzel, M. C., and v R Marais, G. Activated sludge model no. 2. Technical report, IAWQ, 1995.
- Henze, M., Harremoes, P., Jansen, J. C., and Arvin, E. *Wastewater Treatment, Biological and chemical processes*. Springer, 2002.
- Johansen, J. E. and Bakke, R. Enhancing hydrolysis with microaeration. *Water science and Technology*, 2006. 53(8):43 – 50. doi:[10.2166/wst.2006.234](https://doi.org/10.2166/wst.2006.234).
- Kato, M. T., Field, J. A., and Lettinga, G. Anaerobic tolerance to oxygen and the potentials of anaerobic and aerobic cocultures for wastewater treatment. *Brazilian J. Chemical Engineering*, 1997. 14 (4):ISSN 0104-6632. doi:[10.1590/S0104-66321997000400015](https://doi.org/10.1590/S0104-66321997000400015).
- Liden, G., Franzen, C. J., and Niklasson, C. A new method for studying microaerobic fermentations, i). a theoretical analysis of oxygen programmed fermentation. *Biotechnology and Bioengineering*, 1994. 44:419 – 427. doi:[10.1002/bit.260440404](https://doi.org/10.1002/bit.260440404).
- Monod, J. The growth of bacterial cultures. *Annual Review of Microbiology*, 1949. 3:371 – 393. doi:[10.1146/annurev.mi.03.100149.002103](https://doi.org/10.1146/annurev.mi.03.100149.002103).
- Mshandete, A., Börjesson, L., Kivaisi, A. K., Rubindamayugi, S. T., and Mattiasson, B. Enhancement of anaerobic batch digestion of sisal pulp waste by mesophilic aerobic pretreatment. *Water Research*, 2005. 39:1569 – 1575. doi:[10.1016/j.watres.2004.11.037](https://doi.org/10.1016/j.watres.2004.11.037).
- Nguyen, P. H. L., Kuruparan, P., and Visvanathan, C. Anaerobic digestion of municipal solid waste as a treatment prior to landfill. *Bioresource Technology*, 2007. 98(2):380 – 387. doi:[10.1016/j.biortech.2005.12.018](https://doi.org/10.1016/j.biortech.2005.12.018).
- O'Keefe, D. M. and Chynoweth, D. Influence of phase separation, leachate recycle and aeration on treatment of municipal solid waste in simulated landfill cells. *Bioresource Technology*, 2000. 72:55 – 66. doi:[10.1016/S0960-8524\(99\)00089-9](https://doi.org/10.1016/S0960-8524(99)00089-9).
- Pirt, S. J. and Lee, Y. K. Enhancement of methanogenesis by traces of oxygen in bacterial digestion of biomass. *FEMS Microbiology Letters*, 1983. 18:61 – 63. doi:[10.1111/j.1574-6968.1983.tb00449.x](https://doi.org/10.1111/j.1574-6968.1983.tb00449.x).
- Polanco, M. F., Diaz, I., Perez, S. I., Lopes, A. C., and Polanco, F. F. Hydrogen sulphide removal in the anaerobic digestion of sludge by micro-aerobic processes: Pilot plant experience. *Water science and Technology*, 2009. 60(12):3045 – 3050. doi:[10.2166/wst.2009.738](https://doi.org/10.2166/wst.2009.738).
- Reichert, P. *AQUASIM 2.0-User manual; Computer program for the identification and simulation of Aquatic Systems*. Swiss Federal Institute for Environmental Science and Technology (EAWAG), 1998.
- Tang, Y., Shigematsu, T., Ikbal, Morimura, S., and Kida, K. The effects of micro-aeration on the phylogenetic diversity of microorganisms in a thermophilic anaerobic municipal solid waste digester. *Water Research*, 2004. 38:2537 – 2550. doi:[10.1016/j.watres.2004.03.012](https://doi.org/10.1016/j.watres.2004.03.012).
- Weiss, R. F. The solubility of nitrogen, oxygen and argon in water and seawater. *Deep-Sea Research*, 1970. 17:721 – 735.
- Zhou, W., Imai, T., Ukita, M., Li, F., and Yuasa, A. Effect of limited aeration on the anaerobic treatment of evaporator condensate from a sulfite pulp mill. *Chemosphere*, 2007. 66:924 – 929. doi:[10.1016/j.chemosphere.2006.06.004](https://doi.org/10.1016/j.chemosphere.2006.06.004).